Comparing the Structural Stability of PbS Nanocrystals Assembled in fcc and bcc Superlattice Allotropes

Kaifu Bian,[†] Zhongwu Wang,[‡] and Tobias Hanrath*,[†]

[†]School of Chemical and Biomolecular Engineering and [‡]Cornell High Energy Synchrotron Source (CHESS), Cornell University, Ithaca, New York 14853, United States

S *Supporting Information*

ABSTRACT: We investigated the structural stability of colloidal PbS nanocrystals (NCs) self-assembled into superlattice (SL) allotropes of either face-centered cubic (fcc) or body-centered cubic (bcc) symmetry. Small-angle X-ray scattering analysis showed that the NC packing density is higher in the bcc than in the fcc SL; this is a manifestation of the cuboctahedral shape of the NC building block. Using the high-pressure rock-salt/ortho-rhombic phase transition as a stability indicator, we discovered that the transition pressure for NCs in a bcc SL occurs at 8.5 GPa, which is 1.5 GPa higher than the transition pressure (7.0 GPa) observed for a fcc SL. The higher structural stability in the bcc SL is attributed primarily to the effective absorption of loading force in specific SL symmetry and to a lesser extent to the surface energy of the NCs. The experimental results provide new insights into the fundamental relationship between the symmetry of the self-assembled SL and the structural stability of the constituent NCs.

Nature produces a wide variety of materials in which hard crystals are embedded in soft matrices to form complex composites.[1] From skeletal lattices of biological shells to enamel of human teeth and calcite-polymer matrix of ocean sediments, self-assembled soft/mineral composites overcome the fragile weakness of embedded single minerals and strengthen toughness without compromising the materials' hardness.[1b,c,2] Dramatic enhancement of materials' strength enables effective protection from mechanical damage, allowing them to survive harsh natural environments. Earlier studies revealed that the majority of naturally developed biomaterials consist of rich nanoscaled minerals and soft materials that prefer a favorable ratio and self-assemble into order.[1,2] Significant research efforts have been directed at understanding how hierarchical composites with different nanoscopic building blocks lead to enhanced mechanical properties and how these insights can be applied to bio-inspired approaches to the design of novel materials.

Assemblies of colloidal nanocrystals (NCs) provide an analogous complex composite characterized by the hard inorganic crystalline core surrounded by a soft ligand shell. Recent studies by Shevchenko and co-workers showed that the elasticity and hardness of the PbS NC superlattice (SL) resemble the mechanical properties of a polymer, whereas the low fracture toughness reflected the brittle nature of inorganic

materials.[3] These studies also pointed out important remaining unknowns concerning the role and structural organization of the soft organic ligand. Specifically, fundamental structure—property relationships of SLs with different symmetries remain largely unexplored. Inspired by analogous relationships in atomic crystals and natural composites, we set out to determine how and why SL symmetry influences the mechanical stability of the SL and the constituent NCs. In this work, we compare the structural stability of PbS NCs assembled into either fcc or bcc SLs. We discovered that PbS NCs assembled into bcc SLs exhibit higher structural stability, indicated by the higher phase transition pressure. To explain this observation, we investigate several alternative hypotheses and illustrate the how optimized structural arrangement of NCs in the assembly facilitates enhanced structural stability in analogy to complex natural composites.

We recently demonstrated how improved understanding of the NC surface chemistry can be applied to direct the self-assembly of SL allotropes with fcc, bcc, or body-centered tetragonal (bct) symmetry.[4,6] Briefly, up to 60% of ligands on the surface of a PbS NC can be partially removed by exposing the colloidal PbS NC suspension to ambient atmosphere.[4] Based on experimental analysis of the NC surface chemistry and theoretical calculation of the ligand binding energy, we have previously argued that the ligand loss is anisotropic; oleate ligands appear to detach preferentially from {100} facets rather than from neighboring {111} facets. The anisotropic ligand coverage significantly impacts the interaction potential governing the self-assembly of the ordered SLs. NCs with saturated ligand coverage and spherical ligand shell interact isotropically to assemble into an fcc SL. In NCs with reduced ligand coverage, the anisotropic coverage on {111} and {100} facets introduces directionality to the interaction potential, which more closely reflects the cuboctahedral shape of the crystalline core and results in a bcc SL. A similar recent study by Zhang et al. correlated the evolution of PbS NC shape from cubic to quasi-spherical to a continuous transformation of the SL symmetry from simple cubic to rhombohedral phases.[5] An important difference between the fcc and bcc SLs is the orientational order of NCs in their SL sites. NCs in the fcc SL are isotropically distributed; conversely in the bcc SL, the atomic lattice of PbS NCs is coaxially aligned with the [110] growth axis of the bcc SL normal to the substrate.[4,6]

Figure 1 shows transmission electron microscope (TEM) images of the colloidal PbS NCs used to assemble the fcc and
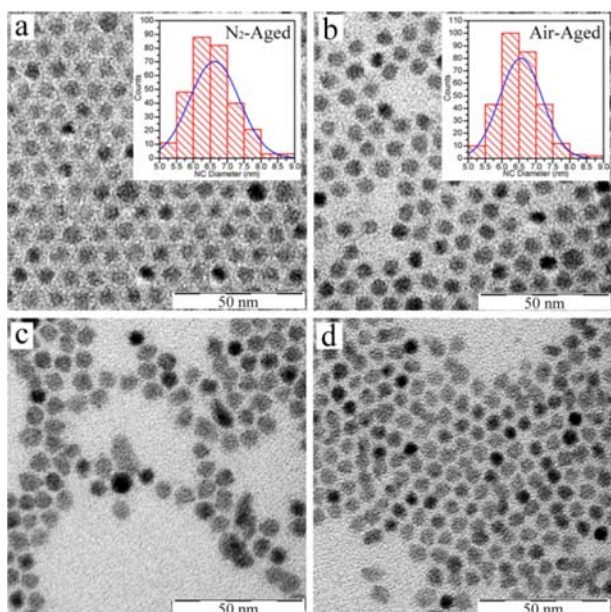

Figure 1. TEM images of PbS NCs (a) aged in nitrogen environment which forms fcc NC SL and (b) aged in air which forms bcc NC SL; insets show histogram of NC diameter distribution. (c) fcc NC SL sample after compression up to 15.5 GPa. (d) bcc NC SL sample after compression up to 16.5 GPa.

bcc SLs in this study. Experimental details including PbS NC synthesis, aging, SL formation, and characterization are provided in the Supporting Information (SI). Statistical analysis of the TEM images confirms that the NCs aged in nitrogen and in air have nearly identical particle diameter and polydispersity, with an average particle diameter of 6.6 nm ($\pm$11%) and 6.6 nm ($\pm$10%), respectively. TEM images of the PbS NCs recovered and redispersed after the high-pressure experiment indicated that the single-particle character of the NCs was preserved. SLs of smaller PbS NCs (d = 3.5 nm) were recently reported to transform into two-dimensional nanosheets at pressures above 11 GPa.[7] Pressure-induced morphology transformations do not appear to occur in the 6.6 nm PbS NCs in this work; this is consistent with the absence of pressure-induced NC fusion reported in the high-pressure experiment by Podsadillo et al.[3a] We note, however, that TEM analysis is restricted to probe a limited fraction of the samples, so we cannot definitively eliminate the possibility of a pressure-induced fusion of part of the NC sample.

Small-angle X-ray scattering (SAXS) patterns at ambient pressure (Figure 2) show that, as expected, PbS NCs aged in nitrogen and air assembled into fcc and bcc SLs with lattice parameters of 13.5 and 10.3 nm, respectively. Importantly, these measurements reveal that the packing density of the bcc SL (1.83 NCs/1000 nm³) is higher than in the fcc SL (1.63 NCs/1000 nm³). The higher packing density of the bcc SL underscores the important relationship between the NC shape and the structure of the SL. Whereas fcc is the most dense packing structure for spherical particles, nonspherical particles can pack into superstructures with higher packing fraction. The dense packing of polyhedral particles is subject to ongoing theoretical and experimental investigation.[8]
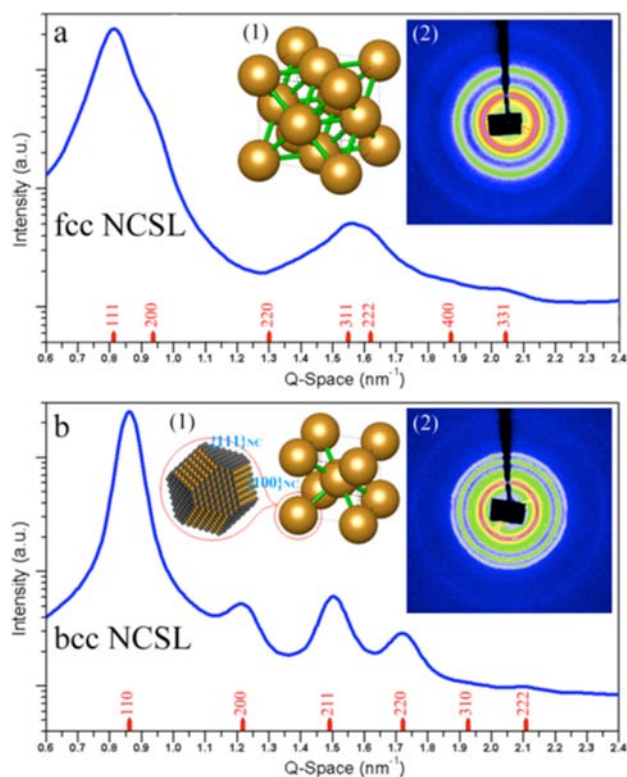

Figure 2. SAXS patterns of (a) fcc (N_2-aged NC) and (b) bcc (air-aged NC) SLs collected at ambient pressure. Insets are the X-ray scattering patterns and illustrations of the corresponding superstructure. Peaks marked in red point out the Miller indices of the SL.

To investigate the structural stability of NCs assembled into different SL allotropes, we turned to pressure-induced transformation of the atomic crystal structure of the PbS NCs. PbS undergoes a pressure-induced phase transformation from the rock-salt ($Fm3m$) symmetry at ambient pressure to orthorhombic ($Cmcm$) symmetry at elevated pressure.[9] The theoretical transition pressure is 9.6 GPa; experimentally determined values range from 2.2 to 2.6 GPa in bulk PbS[9a] and from 8.1 to 9.2 GPa in 7 nm PbS NCs.[3a,7] The phase transition pressure thus provides a convenient experimental marker for the structural stability of NCs. To probe the structural stability of PbS NCs in fcc and bcc SLs, we monitored changes in the X-ray scattering patterns in response to gradually increased pressure in a diamond anvil cell (DAC);[10] a detailed description of the DAC setup and the synchrotron-based X-ray scattering measurements is provided in the SI.

Figure 3 compares the evolution of the wide-angle X-ray scattering (WAXS) patterns of NC in fcc and bcc SLs up to pressures of 15.5 and 16.5 GPa, respectively. Under ambient conditions the PbS NCs exhibit a cubic rock-salt (RS) crystal structure with a unit cell parameter, a_o, of 0.5941 nm, which is slightly larger than the reported spacing in bulk crystals of 0.5924 nm.[11] We indexed the high-pressure phase to the orthorhombic (OR) structure[2a,8c,10,11] with lattice parameters a = c = 0.3887 nm and b = 1.0993 nm. The RS/OR transformation is reversible; reducing the pressure to ambient conditions recovers the RS phase. In the bcc SL, part of the OR phase is preserved at ambient conditions (details in SI). Notably, this discovery points to a possible way to retain a high-pressure metastable phase under ambient pressure by tuning
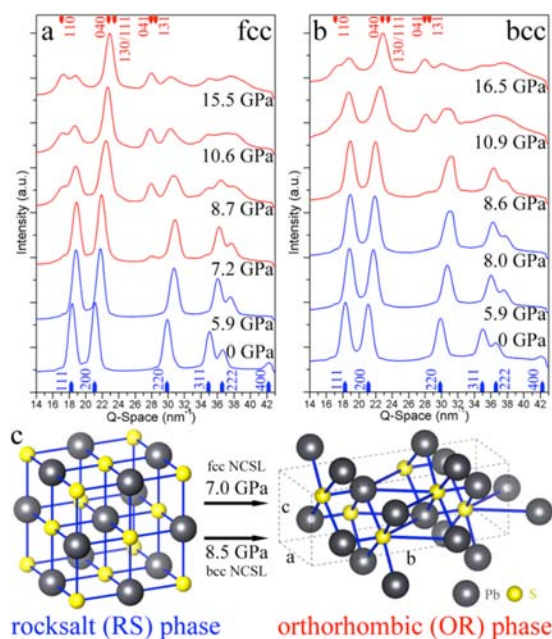
Figure 3. *In situ* high-pressure WAXS patterns of PbS NC SL under compression: (a) fcc and (b) bcc SLs. Peaks marked by arrows represent the Miller indices. Importantly, the phase transition occurs near 7.0 GPa in the fcc SL, whereas for NCs in the bcc SL, the phase transition occurs at higher pressures (8.5 GPa). (c) Schematic of the two PbS crystal structures: left, low-pressure rock-salt (RS) phase; right, high-pressure orthorhombic (OR) phase.

the ordering of the superstructure. We tentatively attribute this hysteresis to residual shear stresses stored in the ligand matrix; experiments to test this hypothesis are currently under way.

Remarkably, PbS NCs assembled into a bcc SL appear to exhibit higher structural stability than similar particles assembled in an fcc allotrope. The pressure-induced RS/OR transformation is observed at 7.0 GPa in the fcc allotrope; similar NCs assembled in a bcc SL, however, are stable at that pressure and only transform to the RS phase at pressures above 8.5 GPa. We have observed this at least 1.5 GPa difference in several sets of high-pressure experiments on PbS NC of similar sizes. Our measurements stand in good agreement with the 8.1−9.2 GPa phase transition pressure of 7 nm PbS NCs reported by Podsadilo et al.[3a] Moreover, we note that he observed difference in transition pressures is significantly larger than the maximum pressure gradient in our DAC, which through careful calibration we have determined to be <0.2 GPa (details in SI). This small gradient does not affect the reliability of the observed 1.5 GPa variation in phase transition pressure in different SL allotropes. This observation leads to the important question: *Why are PbS NCs in a bcc SL more stable than similar particles in a fcc SL?* To answer this question, we have considered several alternative hypotheses, including effect of NC size and surface energy and SL packing density and symmetry.

Earlier work on pressure-induced phase transitions in CdSe NCs by Tolbert and Alivisatos showed that the transition pressure increases with decreasing NC diameter.[9b,c] Since the NCs in bcc and fcc SLs are statistically indistinguishable in size, we can eliminate size-dependent transitions pressures as an explanation. Given that the NCs in bcc and fcc SLs have different ligand coverage, we considered whether the different transition pressures might be due to different surface energies

of the NCs in the bcc and fcc SLs. Unfortunately, quantitative analysis of the surface energies of colloidal NC facets is beyond the capabilities of currently available techniques. However, high-resolution X-ray scattering can provide insights into small changes in the atomic lattice constant, and these changes can be qualitatively related to the surface energy of specific NC facets. As discussed above, we can infer the cuboctahedral shape of the NCs from the Wigner−Seitz construction of the bcc SL. Cuboctahedral NCs are characterized by eight {111} and six {100} facets, as illustrated in the inset of Figure 2b.

Table 1 summarizes the {111} and {200} lattice spacing observed for PbS NCs assembled in bcc and fcc SLs compared

Table 1. *d*-Spacing by WAXS of {111} and {100} Atomic Planes in PbS NC Cores Embedded in fcc and bcc NCSLs under Ambient Pressure

	PbS NCs in fcc NCSL	PbS NCs in bcc NCSL	PbS bulk crystal
$d_{\{111\}}$ (Å)	3.427	3.428	3.420
$d_{\{100\}}$ (Å)	5.948	5.960	5.924
$d_{\{100\}}/d_{\{111\}}$	1.736	1.739	1.732

to the corresponding spacing in bulk PbS.[9a] The measured *d*-spacing of the PbS NC {111} planes stands in good agreement with bulk reported values and shows no significant difference for the bcc and fcc SLs. The *d*-spacing of the {200} planes, however, shows important differences. PbS NCs in both bcc and fcc SLs exhibit an expansion of the {200} lattice spacing compared to the bulk; notably, this effect is significantly more pronounced in the former than in the latter. A lattice expansion relative to the bulk is attributed to a negative surface energy, so the surface energy of the {100} facets of the air-exposed PbS NCs is reduced compared to that for NCs aged in nitrogen. Side-by-side comparison of the surface energy of air-aged PbS NCs in a bcc SL and nitrogen-aged PbS NCs in a fcc SL thus suggests that the NCs with the lower surface energy should be more stable and should exhibit a higher transition pressure, which is qualitatively consistent with the experimentally observed trend.

We calculated the impact of lattice expansion and surface energy on the transition pressure and found that the different surface energies of NCs in fcc and bcc SLs only account for ~1.5 MPa (details in SI). Since the pressure difference is >3 orders of magnitude less than the experimentally observed difference in transition pressure (1.5 GPa), we conclude that surface energy considerations are not the dominant factor for the different stabilities observed in fcc and bcc SLs.

To investigate the possible role of pressure gradients and deviatoric stresses in the bcc and fcc SLs, we considered the differences in packing density and ligand/core ratio. Due to the lower ligand/core ratio and the shape of the core, NCs in the bcc SL are packed more densely than in the corresponding fcc SL. If higher transition pressures observed for bcc than fcc were due to deviatoric stresses within the SL, then the lower transition pressure would be expected in the more densely packed (bcc) structure, which is also opposite to the experimentally observed trend.

Finally, we considered whether the bcc SL with reduced ratio of ligands represents an optimized superstructure and thus enables a preferred absorption of external loading force (i.e., shear stress) by soft ligands to enhance structural stability. To test this conjecture, we calculated the compressibility of SL

volume of bcc and fcc SLs (Figure 4). The results indicate that applied pressure reduces SL volume in bcc 2 times faster than
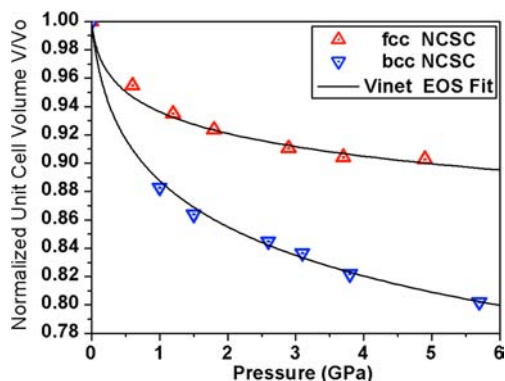

Figure 4. Effect of applied pressure on unit cell volume for fcc and bcc NCSLs. Unit cell volume was normalized with respect to ambient pressure. Red curves are by fitted Vinet equation of state for visual aid (details given in SI).

in fcc. We note that, *in situ*, high-pressure SAXS data confirmed that the symmetry of both fcc and bcc NCSLs did not change under pressure (Figure S5). This clearly indicates that the loading force goes to soft ligands much easier in bcc than in fcc. To understand the relationship between the structural integrity of the NC and the symmetry of the SL, we point a key distinguishing aspect of the fcc and bcc SLs—the orientational ordering. As discussed above, NCs in the fcc SL are isotropically oriented, whereas NCs in the bcc SL exhibit a high degree of orientational ordering. We therefore conclude that the enhanced structural stability of NC in the bcc SL compared to the fcc SL is a direct consequence of the orientational ordering in the former, which is more optimized. Additional experiments reinforced this conclusion: high-pressure X-ray scatterings (Figure S6) of a disordered assembly of the same PbS NCs displayed a phase transition pressure close to that in the fcc SL. These results provide important new insights into the effect of translational and orientational order on the mechanical properties of the SL and the structural stability of the constituent NCs.

In summary, we investigated the structural stability of colloidal PbS NCs assembled into predefined SLs with bcc and fcc symmetry. Using the pressure-induced rock-salt/orthorhombic crystallographic transition as a metric, we found that PbS NCs assembled into a bcc SL exhibit additional stability compared to the same NCs assembled in fcc symmetry. A self-optimized process of surface morphology, energy, and crystallographic orientation of NCs with ligand rearrangement lowers the total free energy of entire ordered nanostructure, resulting in an enhancement of structural stability and mechanical strength. The discovery sheds new light on the formation of nature-tuned hierarchical composites with enhanced and newly manifested properties, thus providing information for design and fabrication of a series of functional materials for technological applications.

ASSOCIATED CONTENT

S Supporting Information

Experimental details concerning the synthesis of PbS NCs; assembly of NCSLs; TEM and SEM characterization; *in situ* X-ray scattering under pressure;and packing density calculations.

This material is available free of charge via the Internet at http://pubs.acs.org.

AUTHOR INFORMATION

Corresponding Author
th358@cornell.edu
Notes
The authors declare no competing financial interest.

ACKNOWLEDGMENTS

REFERENCES

(1) (a) Addadi, L.; Weiner, S. *Nature* **1997**, *389*, 912. (b) Fratzl, P.; Weinkamer, R. *Prog. Mater. Sci.* **2007**, *52*, 1263. (c) Smith, B. L.; Schaffer, T. E.; Viani, M.; Thompson, J. B.; A., F. N.; Kindt, J.; Belcher, A.; Stuckyk, G. D.; Morse, D. E.; Hansma, P. K. *Nature* **1999**, *399*, 761.

(2) (a) Aizenberg, J.; Weaver, J. C.; Thanawala, M. S.; Sundar, V. C.; Morse, D. E.; Fratzl, P. *Science* **2005**, *309*, 275. (b) Eastoe, J. E. *J. Dental Res.* **1979**, *58*, 758.

(3) (a) Podsiadlo, P.; Lee, B.; Prakapenka, V. B.; Krylova, G. V.; Schaller, R. D.; Demortiere, A.; Shevchenko, E. V. *Nano Lett.* **2011**, *11*, 579. (b) Tam, E.; Podsiadlo, P.; Shevchenko, E.; Ogletree, D. F.; Delplancke-Ogletree, M. P.; Ashby, P. D. *Nano Lett.* **2010**, *10*, 2363.

(4) Choi, J. J.; Bealing, C. R.; Bian, K.; Hughes, K. J.; Zhang, W.; Smilgies, D. M.; Hennig, R. G.; Engstrom, J. R.; Hanrath, T. *J. Am. Chem. Soc.* **2011**, *133*, 3131.

(5) Zhang, Y.; Lu, F.; van der Lelie, D.; Gang, O. *Phys. Rev. Lett.* **2011**, *107*.

(6) Bian, K.; Choi, J. J.; Kaushik, A.; Clancy, P.; Smilgies, D. M.; Hanrath, T. *ACS Nano* **2011**, *5*, 2815.

(7) (a) Wu, H.; Bai, F.; Sun, Z.; Haddad, R. E.; Boye, D. M.; Wang, Z.; Huang, J. Y.; Fan, H. *J. Am. Chem. Soc.* **2010**, *132*, 12826. (b) Wang, Z.; Schliehe, C.; Wang, T.; Nagaoka, Y.; Cao, Y. C.; Bassett, W. A.; Wu, H.; Fan, H.; Weller, H. *J. Am. Chem. Soc.* **2011**, *133*, 14484.

(8) (a) Betke, U.; Henk, M. *Comput. Geometry* **2000**, *16*, 157. (b) Torquato, S.; Jiao, Y. *Nature* **2009**, *460*, 876. (c) Haji-Akbari, A.; Engel, M.; Keys, A. S.; Zheng, X.; Petschek, R. G.; Palffy-Muhoray, P.; Glotzer, S. C. *Nature* **2009**, *462*, 773. (d) Henzie, J.; Grünwald, M.; Widmer-Cooper, A.; Geissler, P. L.; Yang, P. *Nat. Mater.* **2011**, *11*, 131−137.

(9) (a) Knorr, K.; Ehm, L.; Hytha, M.; Winkler, B.; Depmeier, W. *Eur. Phys. J. B* **2003**, *31*, 297. (b) Tolbert, S. H.; Alivisatos, A. P. *Science* **1994**, *265*, 373. (c) Tolbert, S. H.; Alivisatos, A. P. *J. Chem. Phys.* **1995**, *102*, 4642.

(10) Quan, Z.; Wang, Y.; Bae, I.; Loc, W. S.; Wang, C.; Wang, Z.; Fang, J. *Nano Lett.* **2011**, *11*, 5531.

(11) Wasserstein, B. *Am. Mineral.* **1951**, *36*, 102.